

Development of a Seismic Design Approach for Infill Walls Equipped with Structural Fuse

Mohammad Aliaari¹ and Ali M. Memari^{*,2}

¹TMAD Taylor & Gaines, 300 N Lake Ave, 14th Floor, Pasadena, CA 91101

²Department of Architectural Engineering, The Pennsylvania State University, 104 Engineering Unit A, University Park, PA, 16802

Abstract: Presented herein is a seismic design approach developed for a proposed infill wall “structural fuse” system for use in building frames. The purpose of this system is to prevent damage to frame or infill walls due to infill wall-frame interaction during potentially damaging earthquakes by isolating them through a “sacrificial” component or a structural fuse. The design approach includes a procedure for design and application of the fuse system in a multi-bay, multi-story building with moment resisting frames. The empirical equation developed to predict the in-plane strength of masonry infill walls equipped with structural fuse is discussed. A calculation method is suggested to specify an appropriate fuse element capacity arrangement in a building frame in order to achieve desirable and controlled structural performance. The design procedure is shown through application to two buildings used for example, a low-rise (4-story) and a mid-rise (8-story) building. The result of the study demonstrates that the proposed isolation system has merits and can potentially improve the seismic performance of masonry infill walls by protecting the infill wall and the frame from damages due to their interaction.

Keywords: Seismic isolation, structural fuse, masonry walls, infill walls, seismic design.

INTRODUCTION

In steel and concrete moment frame construction, infilling some of the interior or exterior bays with walls made of masonry units is a common practice in many countries. In the United States, however, masonry infill walls exist mostly in older buildings. In some new construction masonry infill is used on the exterior frames as the backup wall for brick or stone veneer system as well. Such infill walls are traditionally specified by architects, and structural engineers do not consider them as a participating member in the vertical gravity load-bearing or lateral load-resisting systems. However, depending on their construction details in relation to the structural frame, infill walls can adversely influence the seismic response of the structure and lead to some damage to the wall or frame [1, 2]. Although the philosophy of seismic design is usually based on life-safety issues and not damage prevention aspects, designing to reduce damage is still preferable. Cracking of infill walls, which is a common form of non-structural damage in even minor to moderate earthquakes, can demand expensive repair cost as well as temporary shutdown of normal operation of the building. Stronger earthquakes can lead to total collapse of infill walls with the hazard of falling debris into the streets or interior of buildings. In the Nicaragua 1972 earthquake, it is estimated that

5000 casualties were associated with falling masonry walls and roofs [3]. On the other hand, studies after April 2009 earthquake in the Abruzzo Region of Italy recognized that the masonry infill walls prevented further deterioration or collapse of many buildings [4]. Observation of 1906 San Francisco earthquake also presented relative by superior performance of steel frame structures with masonry infill walls, however, major repairs were required after earthquake [5].

Two methods of construction are common for infill walls [6, 7]. The first method is to allow the infill wall to interact with the structural frame and basically use it as an effective bracing component (*i.e.*, diagonal strut action). The second approach is to isolate the infill wall from the structural frame by leaving gaps between them. In the case of tight-fit construction, the presence of infill walls increases the in-plane stiffness of the structure, decreases its fundamental period, and as a result can generally lead to larger shear forces, primarily during the elastic response phase. Depending on the details of their construction (partial *vs.* complete infill), the infill wall interaction with the confining frame could possibly lead to premature column failure (short column mechanism) or to increased levels of ductility demand in columns. Furthermore, infill walls with tight-fit construction can in general influence the torsional response and sometimes lead to soft-story condition. In the case of separating the infill walls from the frame by leaving gaps between them, issues such as out-of-plane stability of the infill wall, acoustic, and fire insulation requirements at the separation gap need to be addressed.

*Address correspondence to this author at the Department of Architectural Engineering, The Pennsylvania State University, 104 Engineering Unit A, University Park, PA, 16802; Tel: (814) 865-3367; Fax: (814) 863-4789; E-mail: memari@enr.psu.edu

Initial introduction of the Seismic Infill Wall Isolator Subframe (SIWIS) concept by Memari and Aliaari [8] involved the use of a structural fuse element as an alternative method to tight-fit and complete isolation options for infill wall construction that can be classified as a seismic isolation solution with the use of sacrificial fuse elements. The idea is to try to use (to a certain degree) the beneficial effects of strength and stiffness of the infill wall to reduce the story drift during low to moderate seismic events. However, during strong shaking, the sacrificial element should crush and seismically isolate the infill wall from the frame in order to prevent damage to the wall (including cracking) and the frame. The proposed system can be used for seismic retrofit and upgrade of existing and old buildings as well as in new constructions.

To further develop the proposed system and evaluate its performance, a research program including an analytical and an experimental component was undertaken. The development of a generalized nonlinear finite element modeling scheme and an experimental program including a series of compression tests on different types of fuse elements and lateral in-plane static tests on a scaled two-bay, three-story steel frame equipped with structural fuse system has been presented [9-11].

Three different finite element modeling schemes have been used by various researchers for modeling of infilled frames. The first modeling scheme is referred to as micro model [12, 13] to study the stress distribution in the infill wall and its interaction with the confining frame using smeared crack approach with discrete elements. Milani [14] further studied a full three dimensional (3D) modeling of masonry walls using heterogeneous approach for finite element upper bound limit analysis. Besides the detailed micro models, simplified macro models are also used, in which the infill wall is modeled by an equivalent strut such as a nonlinear diagonal spring [12] or equivalent three nonlinear brace elements [15] with force-deformation properties obtainable from testing or the micro model analysis. More detailed information about analytical study of the fuse element including background on various finite element modeling schemes can be found in Aliaari [9] and Aliaari and Memari [10].

The experimental program mainly included a series of static lateral load tests on a scaled two-bay three-story steel frame, with and without fuse element. The main objective of these tests was to experimentally investigate and verify the concept of the proposed fuse system and observe the performance of the whole system and its components (*e.g.*, infill walls, fuse elements, and their connections). It was also intended to provide information to validate finite element modeling schemes. Prior to these frame tests, several other experimental tasks were conducted for in-plane capacity of single masonry wall panels and also for fuse element in three different designs including concrete disk, steel disk, and lumber disk. Complete description and documentation of experimental program is available in Aliaari [9] and Aliaari and Memari [11].

The numerical and experimental results confirmed that the concept of the proposed structural fuse system has merits and works satisfactorily as a "seismic isolation" system. The fuse type element first utilizes the beneficial stiffness and

strength effects of the infill wall up to a predefined point, after which it isolates the infill wall from the frame or limits the participation of infill walls in in-plane resistance.

This paper complements previous published work and introduces a proposed design approach for infill walls equipped with fuse elements (without the need for a subframe initially proposed). First, using available empirical equations in the literature, a series of expressions are developed for estimation of the in-plane strength of masonry walls. The results of an isolated wall panel strength test are compared with the results of developed expressions. Then, a design method is suggested in order to specify appropriate capacity arrangement for fuse elements in a multi-bay, multi-story frame building. Necessary design checks for the confining frame due to infill wall-frame interaction are discussed. The proposed design approach is explained as applied to two hypothetical buildings, a four-story (low-rise) and an eight-story (mid-rise) building in Los Angeles, CA (high seismic zone). The main objectives of developing the examples include demonstrating how the proposed design approach works for practical application and showing the advantages of the proposed system. The scope of the approach developed is limited at this time to lateral loading being considered in only one direction. A more general approach should consider cyclic loading conditions, which is expected to be addressed in follow-up studies based on the results of this study.

SEISMIC STRUCTURAL FUSE CONCEPT

The fuse concept proposed consists of mounting structural fuse elements between infill walls and columns as shown in Fig. (1). Conceptually, the fuse elements can be placed in the vertical components of a subframe system consisting of sandwiched light-gage steel studs (Fig. 1). Within the subframe member at top of the wall, which will not have fuse elements, and in open spaces of the subframe vertical elements, there can be an appropriate flexible filler material for sound insulation and fire-resistance. The infill wall then is to be constructed within the subframe just like a usual masonry wall. The lateral stability of the infill wall will be ensured by out-of-plane restrainers such as brackets and guides usually at top. The location of fuse elements shown near the top of the masonry wall panel in Fig. (1) is chosen because the frame will first contact the infill wall at that point and will tend to close the gap if there were no fuse elements. To provide flexural stability and eliminate flexural failure of masonry wall in fuse-equipped system, vertical components of the subframe (in the initial concept of using subframe) attached at each end of the wall panel act as a tie-down element. Other equivalent tie-down concepts can be used if such subframe is not to be employed. In case a subframe is not to be used, the fuse element can be fitted within a small space on the wall edge by using a partial masonry unit or leaving one unit out as shown in Fig. (2). It is envisioned that the fuse element used in this fashion will be enclosed and protected against environmental effects, *e.g.*, moisture and thus the deterioration will be minimized. Nonetheless, in case of any kind of damage due to material breakdown after long time or due to breakage under interaction loads, *i.e.*, performing its fuse function, the detail to be developed (*e.g.*,

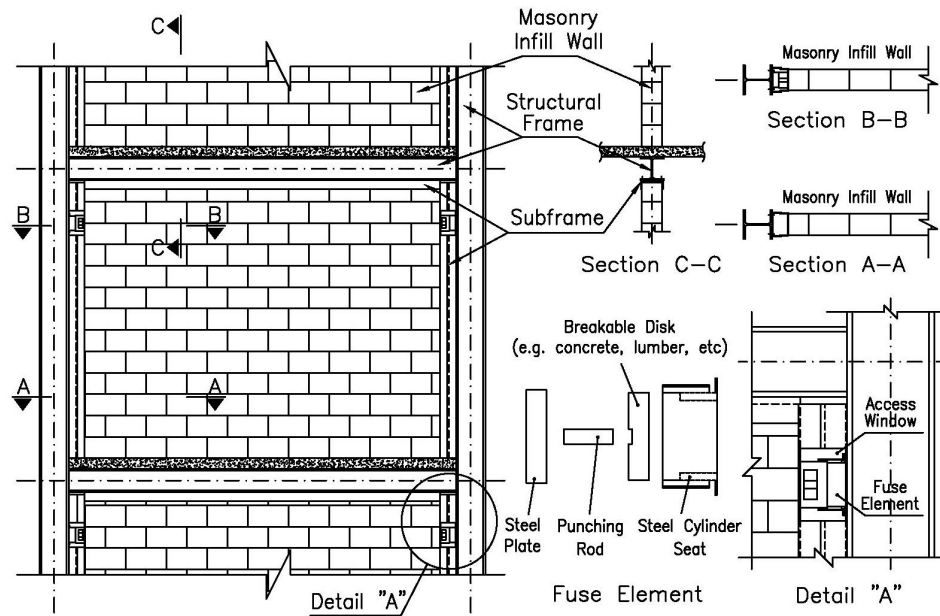


Fig. (1). An example of fuse-equipped system used in a building frame.

as shown in Fig. 2) should allow replacement of the fuse element.

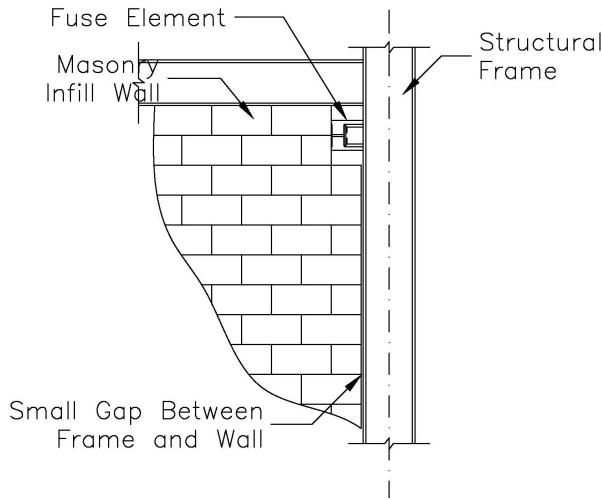


Fig. (2). Example of fuse detail without the use of subframe.

The fuse-equipped system is designed such that under small to moderate levels of structural frame in-plane interface force (low to moderate seismic event or wind), the fuse will act as a rigid link and transfers the force to the infill wall for the benefit of its stiffness in reducing drift. Such reduction in drift can prevent damage to nonstructural components such as glazing, plaster, drywall, veneers, and ornamental components attached to the building façade. At larger levels of in-plane force (moderate to high seismic event), the fuse elements will likely crush (break) after its capacity is overcome by the frame-wall interaction force and allow the structural frame to displace without transferring force to the infill wall. Depending on the stiffness and strength of the masonry wall and the level of confidence in the wall material, its strength, and the desired safety factor, the capacity of fuse element can be customized and different grades can be de-

signed and specified. The upper bound capacity of the fuse element needs to be lower than the lower bound strength of the masonry wall. Consideration needs to be given whether the designer is willing to accept some masonry wall damage or desires little or no damage. The fuse system can be used with different configurations of masonry infill walls including walls with or without openings, partial-height or full-height infills, and infills with different types of masonry units ranging from higher strength concrete masonry blocks and clay brick units to lower strength masonry such as thin wall hollow clay tile units and autoclaved aerated concrete (AAC) blocks.

The early concept of the fuse element intended to make a rigid-like connection between the infill wall and the frame to engage the infill wall in in-plane load resistance up to a certain load level. Accordingly, once this load limit is exceeded, the fuse element will crush and result in full or partial disengagement of the infill wall from interaction with the frame. The capacity of the fuse element is designed to be a percentage of the cracking load of the infill wall, with the percentage reflecting the desirable safety margin. The fuse element discussed in this study is that of the initial concept and has no tension resistance capacity. There could be various design alternatives for fuse element. For example, the fuse element can include a spring component of desirable stiffness to control in-plane movements after the crushing of the fuse element. Furthermore, a dashpot mechanism can be added to the element to enhance seismic performance of a structure by increasing its energy dissipation capacity.

Depending on the type and material of fuse element, its material deterioration and possible impact on long term performance and capacity of the fuse system need to be considered and evaluated. If common structural materials such as concrete, steel, wood and some types of epoxies are used, it is expected that the fuse element maintains its capacity and performance during the life of fuse system, considering the fact that the element will be located inside subframe or upper

corner block (Fig. 2) and further more protection against weather and water can be provided by wall covers, if any, such as gypsum boards or other architectural elements. However, if for any reason (e.g., the nature of the material used) the capacity of fuse elements deteriorates by time, this will not create life safety problems or concerns. The whole concept of fuse system is to disengage the infill wall from structural frame under certain threshold load level, after which the structural frame will provide serviceability and strength requirements as per structural codes and standards. The fuse elements can be investigated after any major event and if needed they can be replaced through accesses in subframe. Depending on the material, it might be appropriate to specify a life limit for fuse elements as well, after which they all need to be replaced. In case the fuse loses strength for reasons such as rot, material useful life, or any other factor not considered in detail, the fuse simply breaks at a smaller load and leads to elongation of the natural vibration period of the entire system, but it should not affect the structural strength after fuse breakage.

In this paper, only brittle type fuse element is considered and the design procedure presented is shown for application of rigid-brittle element. Follow-up studies are expected to include fuse elements with tension and compression resistance as well as possibly energy dissipating properties. One example of such fuse element is to use wood disk as shown in Fig. (3) [11]. The figure shows how the wood disk is punctured by a steel rod if frame-to-wall transfer forces exceed the wood disk capacity.



Fig. (3). Example of a fuse element consisting of a wood disk after steel rod punctures the disk.

IN-PLANE STRENGTH OF MASONRY WALLS USING EMPIRICAL EQUATIONS

Over the last two decades a considerable amount of new research has been carried out on in-plane behavior of masonry walls including experimental and analytical studies. Several researchers have proposed different empirical equations to estimate the in-plane strength of masonry walls [6, 16 - 28]. The results of either experimental tests or analytical studies or both have been used to validate the proposed equations. Empirical equations are commonly used in building design codes for simplicity and practical purposes. For in-

stance, Uniform Building Code [29], Eurocode [30], NEHRP [31], and International Building Code [32] that refer to Building Code Requirements for Masonry Structures [33] have adopted such equations for nominal strength of masonry walls.

Some of the empirical equations proposed by different researchers and building codes for predicting the in-plane strength of masonry walls (V) are summarized in Table 1. The Eurocode [30] equation in the table is based on sliding shear failure, while the rest of the equations are based on diagonal shear failure. Each equation includes two or more of the components listed in Equation (1) below, in which, V_m , V_p , V_{sh} , and V_{sv} , respectively, are the contributions of masonry, axial compression, horizontal reinforcement, and vertical reinforcement.

$$V = V_m + V_p + V_{sh} + V_{sv} \quad (1)$$

The in-plane strength given by the empirical equations listed in Table 1 is compared in the next section with the test results to develop a new series of expressions for in-plane strength of a masonry wall to be used for infilled frames with fuse elements.

Unlike shear resistance, relatively accurate methods are available to calculate the in-plane flexural resistance of masonry walls. One such method has been presented by Tomazevic and Lutman [28] that assumes a symmetrical vertical reinforcement arrangement along the horizontal cross section of masonry walls. Accordingly, Equations (2) and (3) are obtained for the in-plane flexural capacity (M_n) and associated shear resistance (V) of masonry walls based on boundary conditions.

$$M_n = \frac{\sigma_c t L^2}{2} \left(1 - \frac{\sigma_c}{\kappa f'_m} \right) + (L - 2d') A_{sv} f_{yv} \quad (2)$$

$$V = \frac{M_n}{\psi' H} \quad (3)$$

In Equation (2), σ_c is the axial compression stress, f'_m is compressive strength of masonry, f_{yv} is vertical steel yield strength, L is horizontal distance between tie-down element and jamb, t is wall thickness, d' is the centroidal distance of the vertical steel to the nearest jamb, and A_{sv} is the vertical steel area. κ is a coefficient that takes into account the vertical stress distribution at the compressed toe. A common assumption is an equivalent rectangular stress block with $\kappa = 0.85$. In Equation (3), H is the total height of the wall panel and ψ' equals 0.5 for fixed ends walls and 1.0 for cantilever walls.

IN-PLANE STRENGTH OF MASONRY WALLS IN PROPOSED SEISMIC FUSE SYSTEM

The proposed fuse system is intended to prevent masonry infill walls from experiencing damage in strong earthquake activities. A fuse-like element should always disengage the masonry wall from the frame well before the wall reaches its damaging state. For the purpose of fuse element design, the

Table 1. Empirical Equations for In-plane Shear Resistance of a Masonry Wall (1in. = 25.4 mm, 1 kip = 4.448 KN)

Source	Masonry, V_m	Axial Compression, V_p	Horizontal Steel, V_{sh}	Vertical Steel, V_{sv}
[18]	$0.012k_o f'_m A$	$0.2\sigma_c A$	$0.011k_o \gamma \delta \rho_h^{0.31} A f_{yh}$	$k_o k_{sl} \left[\left(\frac{0.5}{r+0.8} \right) + 0.18 \right] \sqrt{f'_m f_{yv} (\rho_v)^{0.7}} A$
[26]	$c_2 \sqrt{f'_m} A$	$c_1 \sigma_c \sqrt{f'_m} A$	$\left[\left(\frac{L-2d'}{s} \right) - 1 \right] A_{sh} f_{yh}$	$c_1 \rho_v f_{yv} \sqrt{f'_m} A$
[27] ^a	$C_1 f'_m \sqrt{1 - \frac{C_2 \sigma_c}{f'_m}} A + C_3 \sigma_c A$		$C_5 \left[\frac{l-2d'}{s} - 1 \right] A_{sh} f_{yh}$	$C_3 C_4 \rho_v f_{yv} A$
[35]	$0.02 f'_m \psi A$	$f'_m \left[0.88 \left(\frac{\sigma_c}{f'_m} \right) - 0.9 \left(\frac{\sigma_c}{f'_m} \right)^2 \right] \psi A$		
[28] ^b	$\left(\frac{f_t}{b} \right) \sqrt{1 + \frac{\sigma_c}{f_t}} A$		$\Phi_h A_{sh} f_{yh}$	
[6] ^c	$\left(\frac{f_t}{b} \right) \sqrt{1 + \frac{\sigma_c}{f_t}} A$		$C_{rh} 0.9d \frac{A_{sh}}{s} f_{yh}$	$\sum 0.806d_{rv}^2 \sqrt{f'_m f_{yv}}$
[29]	$C_d \sqrt{f'_m} A_e$		$\rho_h A_e f_{yh}$	
[31,33] ^d	$c_3(4-1.75\alpha_v) \sqrt{f'_m} A$	$0.25\sigma_c A$	$0.5d \frac{A_{sh}}{s} f_{yh}$	
[30]	$\tau_o A$	$0.4\sigma_c A$	$0.9A_{sh} f_{yh}$	

Notes:

^a Based on regression analysis on the results of a parametric finite element study, Shing *et al.* [27] proposed $C_1=0.04$; $C_2=4.5$; $C_3=0.25$; $C_4=0.667$, and $C_5=0.75$.

^b Tomazevic and Lutman [28] proposed $\Phi_h = 0.4$ based on the experimental results.

^c According to Tomazevic [6], C_{rh} can vary between 0 and 0.5 with a proposed value of 0.3 in the case of lack of experimental results.

^d α_v needs not to exceed 1.0. There is a maximum $V_{max} = 6A\sqrt{f'_m}$ for $\alpha_v < 0.25$ and $V_{max} = 4A\sqrt{f'_m}$ for $\alpha_v < 1.0$.

damaging limit state can be defined to be either initial cracks or major cracks of masonry wall. The initial and major cracking capacity of a masonry wall can be approximated to be about 40% and 70% of its ultimate capacity, respectively [6, 34]. Thus, the ultimate capacity (strength) of a masonry wall to employ fuse system needs to be estimated. The ultimate capacity of an unreinforced masonry wall is the smaller of its shear and flexural capacities. It is often preferred to eliminate the in-plane flexural induced uplift failure of a masonry wall. This can be addressed in the proposed fuse device by providing sufficient strength and stiffness for a vertical element that anchors the wall to the bottom (beam) support such as tie-down at the wall boundary like a jam element. The tie-down element ensures that flexural failure will not occur in masonry wall.

In this section, the in-plane strength of masonry wall is estimated with the use of empirical equations. For this purpose, first, the empirical equations listed in Table 1 are used to predict the strength of a single masonry wall that had been tested as part of this study. Then, those equations that yield closer results are considered and used to develop a new series of expressions for in-plane strength of a masonry wall to be used in infilled frames with fuse elements.

Two single-layer masonry brick walls were constructed and tested as part of an experimental program in this study. Fig. (4) shows the free body diagram of the masonry wall panel as configured in the experimental test. The walls had nine-course running bond with four bricks in each course resulting in a total height of 24-1/4 in. (616 mm), a total length of 32 in. (813 mm), and an actual thickness of 3-1/2 in. (89 mm). The failure mode for both wall specimens was diagonal shear failure. Both wall specimens failed in brittle manner right after the formation of the first cracks, which were developed simultaneously. They failed in diagonal shear mode at maximum loads of 22.3 kips (99.2 KN) and 24.3 kips (108.1 KN). Thus, an average of 23.3 kips (103.6 KN) was considered for the in-plane strength of the wall specimen. The compressive test on three masonry prisms resulted in a compressive strength of $f'_m = 3600$ psi (24.9 MPa) for masonry. The details and complete discussion of these wall tests have already been reported by Aliari [9].

The tensile strength of masonry is required for use in some of the empirical equations listed in Table 1. In the case of lack of test results, the tensile strength of masonry can be approximated based on the compressive strength of masonry.

Based on analysis of data from a large number of test results by Tomazevic [6], the ratio between the tensile and compressive strength of masonry varies from 0.03 to 0.09 with an average of 0.05. The use of the average value of 0.05 results in a tensile strength of $f_t = 180$ psi (1.25 MPa) for the masonry material of the case under study (for $f'_m = 3600$ psi).

With reference to Fig. (4), by taking moment about the bottom-left corner, Equation (4) is obtained for the axial load N (tie-down load) based on the applied horizontal load V , where, l , l' , h , and h' are dimensions shown in Fig. (4). The assumption of $l' \approx 0.05l \sim 0.10l$ and $h' = 0.05h \sim 0.10h$ and the substitution of $\sigma_c = N/A$ in Equation (4) result in Equation (5) for the average compressive stress.

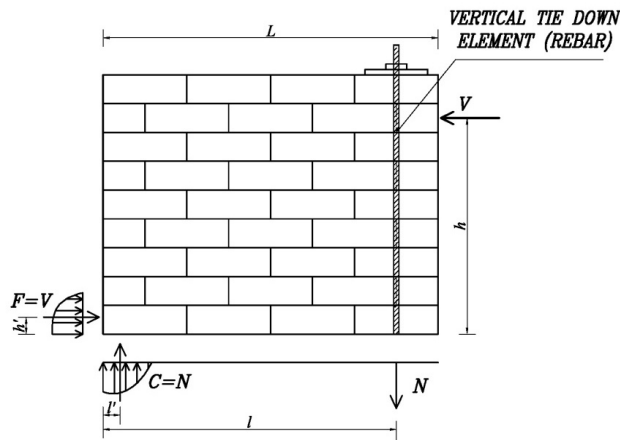


Fig. (4). Masonry wall panel subjected to in-plane load.

$$N = \frac{h - h'}{l - l'} V \tag{4}$$

$$\sigma_c = \frac{h}{lA} V \tag{5}$$

The empirical equations listed in Table 1 are considered here for in-plane shear strength prediction of the test wall specimen. For each empirical equation, σ_c was substituted by Equation (5) and the resultant equation was solved for V . The resulting in-plane resistances (V) for the test masonry wall specimen including shear resistance, flexural resistance, and test result are shown in Fig. (5) for comparison. As an example, the calculations based on the equation by Tomazevic and Lutman [28] are summarized as follows:

$$\sigma_c = \frac{h}{lA} V = \frac{24.25 - 4}{28(32 \times 3.5)} V = 0.0065V$$

$$V = \left(\frac{f_t}{b}\right) \sqrt{1 + \frac{\sigma_c}{f_t} A} = \left(\frac{180}{1}\right) \sqrt{1 + \frac{0.0065V}{180} (32 \times 3.5)} = 20160 \sqrt{1 + \frac{V}{27690}}$$

$$\implies V = 28.8 \text{ kips (128.1 kN)}$$

It can be seen from Fig. (5) that the flexural strength of the wall is about two times the shear strengths. This is of

course desirable since it allows the full capacity of masonry material to be used and eliminates flexural failure of masonry walls. Fig. (5) shows that the Fattal [18] and UBC 1997 [29] equations resulted in highly conservative values. The Fattal [18] equation was primarily developed to estimate the shear resistance of reinforced masonry walls and, thus, it is not suitable for unreinforced masonry walls. Although the UBC 1997 [29] equation was entitled as “nominal shear strength” of masonry walls, but it was basically developed for design purposes. Furthermore, the UBC 1997 [29] equation lacks the terms related to the resistance of the axial compressive stress. Therefore, it is predictable that this equation may result in conservative values. The Shing *et al.* [26] equation also resulted in lower resistance compared to the test result. However, the Shing *et al.* [27] equation gave better results. The other three equations including Tomazevic and Lutman [28], Guqiu *et al.* [35], and NEHRP [31] and Building Code Requirements for Masonry Structures [33] predicted the presented test results fairly well.

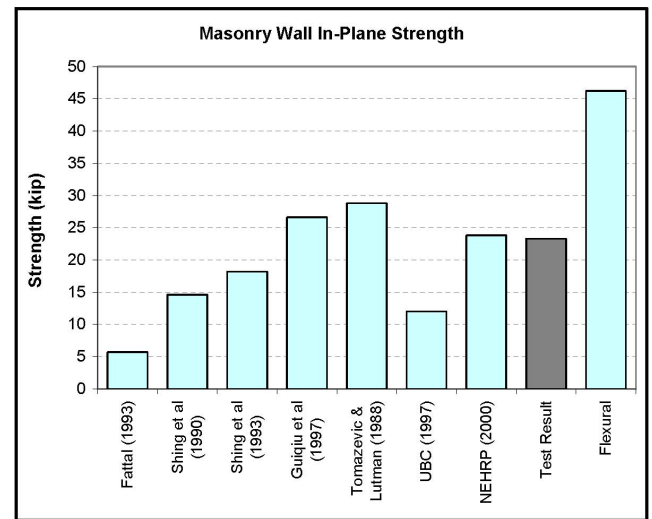


Fig. (5). In-plane strength of masonry wall test specimen (1 kip = 4.448 KN).

In this study, empirical equation proposed by Tomazevic and Lutman [28] is considered as shown in Eq. (6), in which f_t is tensile strength of masonry, b is a factor related to aspect ratio of wall, A_{sh} and f_{yh} are area and yield strength of horizontal rebar, σ_c is axial compression stress and Φ_h is reduction factor for contribution of rebar capacity.

$$V = \left(\frac{f_t}{b}\right) \sqrt{1 + \frac{\sigma_c}{f_t} A} + \Phi_h A_{sh} f_{yh} \tag{6}$$

Substitution of σ_c from Eq. (5) into Eq. (6) and solving for V results in Eq. (7) for in-plane resistances (V) for the masonry wall in fuse system, in which $\beta = h/l$. Use of this equation will be illustrated subsequently through examples.

$$V = Af'_m \frac{\beta}{40b^2} \left[1 + \sqrt{1 + \frac{4b^2}{\beta^2}} \right] \tag{7}$$

GUIDELINES FOR FUSE ELEMENT CAPACITY ARRANGEMENT

In a typical multi-story building earthquake induced drifts cause larger story shear forces in lower stories relative to upper stories. Thus, if the same capacities are used for fuse elements in all stories, those in lower stories will fail first. This sequence of crushing of fuse elements can result in development of a soft-story, which is an unfavorable mechanism for the structure. A desirable sequence of crushing of fuse elements can be obtained by specifying fuse elements with different capacities (grades) in elevation. In this section, a method is developed to design fuse elements' capacity arrangement in multi-bay, multi-story buildings to achieve desirable structural performances and prevent soft-story mechanism [37].

A multi-bay, multi-story frame subjected to in-plane lateral loads is shown in Fig. (6). The story shear force is the sum of the applied loads at and above the story under consideration as shown in Eq. (8).

$$V_{i-reqd} = \sum_{j=i}^n F_j \tag{8}$$

On the other hand, the story shear resistance is the sum of the resistances of masonry infill walls equipped with fuse elements, the resistance of frame, and the resistance of bracings as shown in Eq. (9). The share of the resistance of each term is proportioned to their relative stiffness values.

$$V_{i-total} = V_{i-wall} + V_{i-frame} + V_{i-brace} \tag{9}$$

With the distribution of the required story shear forces in elevation (V_{i-reqd}) known, to achieve a desirable crushing sequence of fuse elements in elevation, the capacities should be specified in such a way that the ratios of the provided story shear resistance ($V_{i-total}$) to required story shear forces (V_{i-reqd}) follow the preferred crushing sequence. Since it is usually desirable for fuse elements to crush from top stories to the bottom, these ratios should be in increasing order from

top to bottom stories. To illustrate the design method based on this assumption, two design examples are presented subsequently.

CONSIDERATIONS FOR INFILLED FRAME DESIGN

In the proposed infill wall fuse system concept, the frame and the wall panel interact at the locations of fuse element, vertical tie-down element, and the compression toe of wall panel. These interactions affect the bending moment, axial force, and shear force of the frame (global effects) and need to be checked by the designer. After the fuse element crushes (breaks), there will be no interaction between the frame and the wall, and the frame will act as a bare frame. Fig. 7(a) shows the qualitative bending moment and shear force diagrams of a bare frame subjected to an in-plane load. The bending moment and shear force diagrams induced due to the presence of a fuse device is also shown in Fig. 7(b). The response of the frame is considered to be linear before crushing of the fuse elements. Thus, with the use of superposition principle, the resulting resisting forces of the frame are the sum of the forces of the bare frame and those induced by the fuse system on the frame as shown in Fig. 7(c). In Fig. (4), for simplification purposes, the distributed compression stress at the compression toe of the wall is substituted by an equivalent concentrated force. For analysis and design purposes of a structural frame with a fuse system, it is appropriate to substitute the effects of fuse system as new load cases by considering its reaction on the confining frame.

Another design consideration for the frame is to check the column and beam members' concentrated forces for local effects (e.g., flange or web buckling) fuse system interaction. The column experiences concentrated compressive force from the fuse at the location of the fuse element, which translates to show shear force on column, and the bottom beam is subjected to concentrated shear force due to the tensile force at the location of the tie-down element. The beam is also subjected to compressive force at the compression toe of the wall. These global and local effects and reactions need to be considered when checking and designing the frame elements.

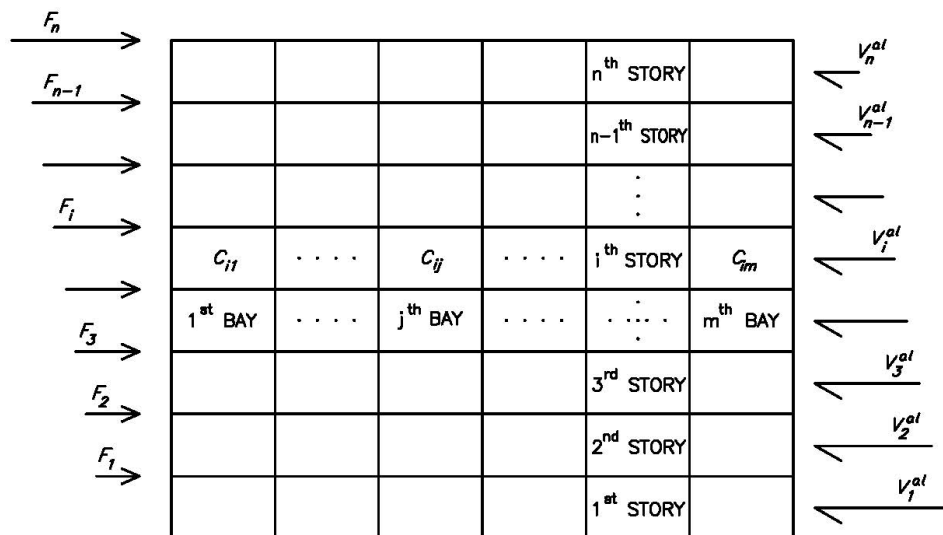


Fig. (6). Multi-bay multi-story building subjected to in-plane loads.

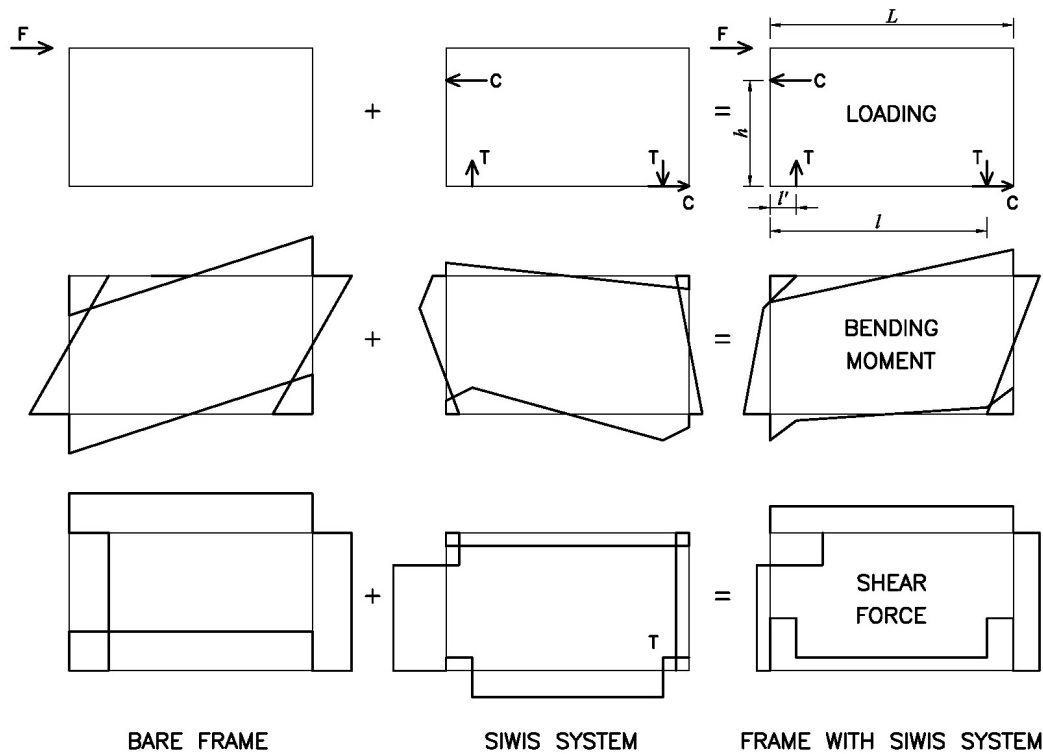


Fig. (7). Influence of infill wall fuse system in frame forces.

Table 2. Eight-story Building Design Example

Story	Story Shear kip (KN)	Story Shear Ratio	Fuse Capacity Kip (KN)	Story Shear Capacity Kip (KN)	Story Capacity / Story Shear	Fuse Crushing Sequence	Fuse/Wall Capacity %
(1)	(2)	(3)	(4)	(5)	(6)	(7)	(8)
8	112 (498)	NA	10 (44)	40 (178)	0.36	1	11
7	205 (911)	1.84	25 (111)	100 (445)	0.49	2	28
6	282 (1254)	1.37	40 (178)	160 (712)	0.57	3	44
5	343 (1526)	1.22	55 (245)	220 (979)	0.64	4	61
4	389 (1730)	1.13	65 (289)	260 (1156)	0.67	5	72
3	420 (1868)	1.08	75 (334)	300 (1334)	0.71	6	83
2	439 (1953)	1.04	85 (378)	340 (1512)	0.77	7	94
1	447 (1988)	1.02	90 (400)	360 (1601)	0.81	8	100

DEVELOPMENT OF THE DESIGN APPROACH THROUGH EXAMPLES

Two hypothetical design examples are presented in this section to help explain the fuse system design procedure. An eight-story building consisting of regular frames with equal bay sizes and a four-story building with different bay and story sizes and partial infill walls are considered to be located in Los Angeles, CA for evaluating the performance of the infill wall with fuse system in a high seismic zone. The seismic design forces are calculated using ASCE 7 [36] assuming normal conditions, e.g., Seismic Use Group I, Site

Class C, and R=8 (special steel moment resisting frame system) for the eight-story, and R=4.5 (intermediate steel moment resisting frame system) for the four-story building.

Example 1: Eight-Story Building

A hypothetical eight-story office building with the plan area of 80 feet (24.38 m) by 75 feet (22.86 m) and the story height of 12 feet (3.66 m) as shown in Fig. (8) serves as the first example. A total gravity load of 150 psf (7.18 kN/m²) is assumed for all levels. The longitudinal direction of this building with 4 bays is considered here. A masonry infill

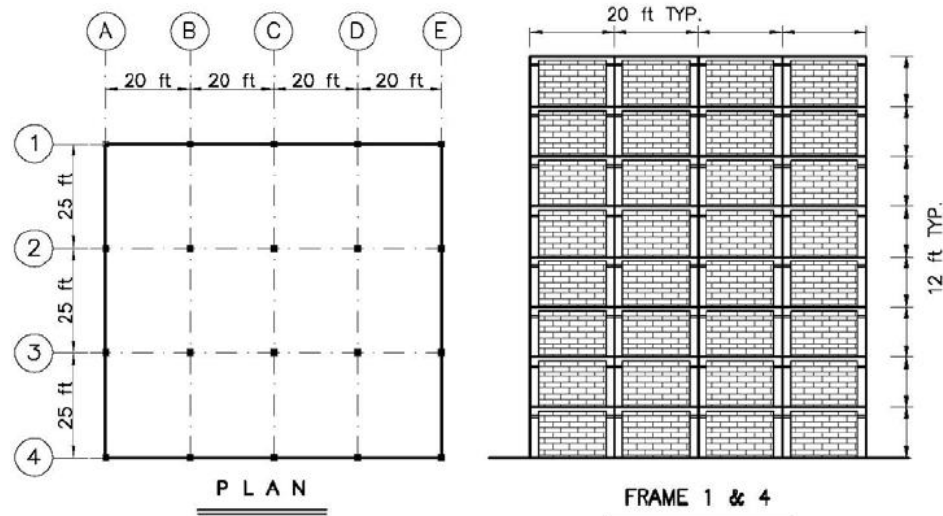


Fig. (8). Eight-story office building example (1 in. = 25.4 mm).

wall with 8 in. (203 mm) thickness and a masonry tensile strength of 125 psi (0.86 MPa) are assumed for all panels (considered medium wall). Eq. (7) was used for in-plane strength estimation of masonry walls. The initial cracking load of the masonry wall panel (taken as 40% of the ultimate resistance) is assumed to be the limiting criterion for the capacity of fuse element. Eq. (10) can be obtained from Eq. (7) for the maximum capacity of fuse elements, C_{max} , by substituting $f_t = 0.05 f'_m$ as discussed earlier and using a safety factor (SF) as follows:

$$C_{max} = \frac{0.2 \beta A f_t}{SF b^2} \left[1 + \sqrt{1 + \frac{4b^2}{\beta^2}} \right] \tag{10}$$

A safety factor (SF) of 1.25 is assumed for this example. Eq. (10) results in a maximum capacity of 90 kips (400 kN) for the fuse elements to be used. The seismic story shear forces for one longitudinal frame are calculated and summarized in Table 2 (2nd columns). For the steel moment resisting frame, the resistance term related to the moment frame can be neglected in this example for simplicity, since the in-plane stiffness of the steel frame columns is small compared to the in-plane stiffness of all the masonry wall panels [37]. Thus, Eq. (11) can be obtained from Eq. (9) as follows:

$$V_{i-total} = V_{i-wall} = \sum_{j=1}^m C_{ij} \tag{11}$$

In order to determine a suitable capacity distribution for fuse elements in elevation (various stories), the ratio of seismic story shear force for each story to that for the above story is calculated and listed in Table 2 (3rd column). For instance, the value of 1.22 results for the 5th story by dividing the 5th story shear force (343 kips (1526 kN)) by the 6th story shear force (282 kips (1254 kN)). These ratios are used to determine the distribution of fuse element capacities in elevation as discussed earlier to derive the preferred sequence of crushing of fuse elements. Since the preferred sequence of crushing of fuse elements will be top to bottom in

a building, the ratios of fuse element capacities, V_{i-wall} , in elevation should exceed the calculated ratios of story shear forces listed in Table 2 (3rd column). The appropriate capacities of fuse elements are determined and listed in Table 2 (4th column) as subsequently explained for various stories.

Since a maximum wall strength of 90 kips (400 kN) was determined, a capacity of 90 kips (400 kN) is assumed for the 1st story's fuse elements such that it is smaller than the shear capacity of the masonry infill wall. The desirable maximum capacity for the 2nd story's fuse elements is determined by dividing the assumed capacity of fuse elements in the 1st story, which is 90 kips (400 kN), by the calculated story shear ratio for the 1st story, which is 1.02. This results in a capacity of 88 kips (391 kN). Thus, if the capacity of fuse elements in the 2nd story is taken to be smaller than 88 kips (391 kN), those elements will be expected to crush before the fuse elements of the 1st story, which is desirable to eliminate soft story mechanism. To designate capacities in multiples of 5 kips (22 kN), a capacity of 85 kips (378 kN) is assumed for the 2nd story's fuse elements. Similarly, for the 3rd story, the desirable maximum capacity is 85 kips/1.04 = 81 kips (360 kN), thus a capacity of 75 kips (334 kN) is assumed. The result of this procedure, which is listed in Table 2 (4th column), completes the selection of the required fuse element capacities.

To verify this design, the sequence of crushing of fuse elements in elevation is checked next. The sum of fuse element capacities for each story is calculated by multiplying the capacity of each element (4th column) by the number of bays in each story as listed in Table 2 (5th column). This is for the case of using the same capacity for fuse elements in all bays of a given story. The ratio of story fuse elements capacity (5th column) to the story shear force (2nd column) is calculated and listed in Table 2 (6th column). The sequence of crushing of fuse elements in elevation can be determined by comparing the order of these ratios in Table 2 (7th columns), which shows that the crushing sequence is from top to bottom, as designed.

The information in Table 2 implies that for this eight-story building example, the specified fuse elements crush under the design seismic loads to protect cracking and failure of masonry infill walls. The 8th story's fuse elements crush first at 36 percent of the total seismic design load. The fuse elements of the 1st story crush last at 81 percent of the total seismic design load. Thus, if a weaker earthquake with effects less than 36 percent of the design earthquake occurs, none of the fuse elements will be expected to crush. In the last column in Table 2, the ratio of fuse element capacity to the masonry infill wall cracking capacity (90 kips (400 kN)) is calculated for each story. These ratios indicate the percentage of masonry wall capacity under which the designed fuse elements are expected to break and imply the beneficial effects of the masonry walls being effectively used. For instance, under design seismic loads, the walls of the 8th, 4th, and 1st stories become isolated at their 11, 72, and 100 percent capacities, respectively. In other words, the masonry walls of the 4th story contribute to the lateral resisting system until the walls experience 72 percent of their capacities; afterward, they are disengaged by crushing of fuse elements.

It can be concluded for this example that low to moderate earthquakes will not cause the fuse elements to crush. In moderate to strong earthquakes, some of the upper stories fuse elements will crush, while they will all crush in a strong earthquake event. For instance, it can be predicted from Table 2 that if an earthquake equivalent to 70 percent of the design earthquake occurs, only the fuse elements of top five stories (the 8th, 7th, 6th, 5th, and 4th stories) will crush. This example demonstrates that the proposed fuse system can act as intended to minimize the possibility of the masonry walls getting cracked and the frame experiencing premature failure in earthquakes. At the same time, this system can use the beneficial effects of masonry walls in a controlled (pre-determined) manner.

Example 2: Four-Story Building

To illustrate the effects of variations in bay size and infill height (e.g., partial height), a four-story hypothetical building as shown in Fig. (9) is considered next. The structural system includes an intermediate steel moment resisting frame system (R=4.5). The plan area is 75 feet (22.86 m) by

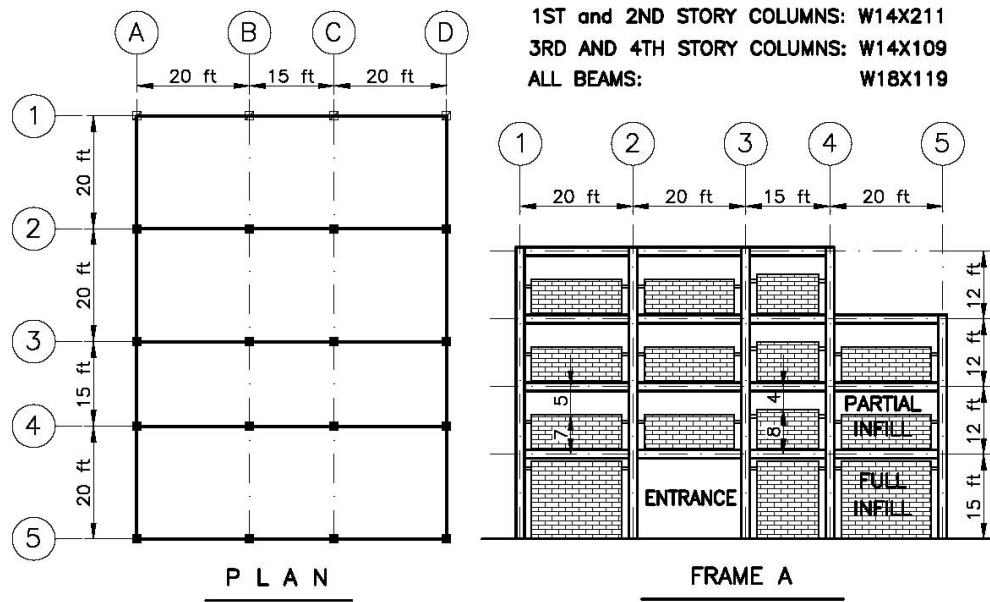


Fig. (9). Four-story building example (1 in. = 25.4 mm).

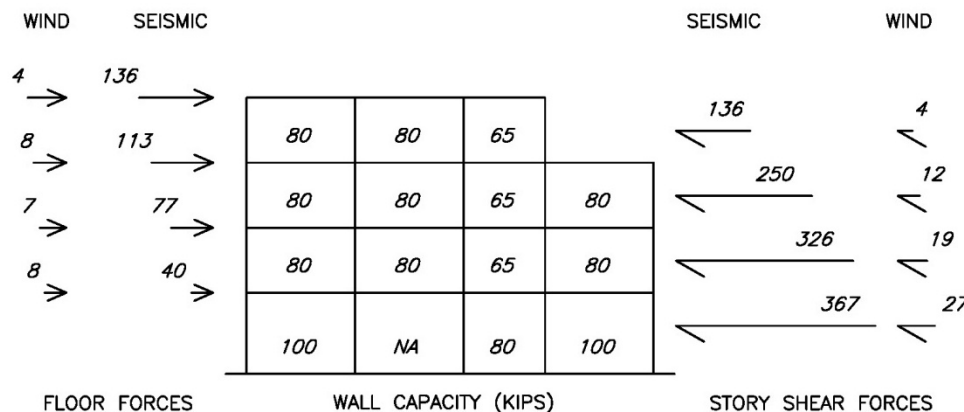


Fig. (10). Applied seismic loads and wall capacities for four-story building example (1 kip = 4.448 kN).

55 feet (16.76 m) and the story heights are 15 feet (4.57 m) for the first story and 12 feet (3.66 m) for the next three stories. The longitudinal direction of this building with 4 bays is assumed for analysis in this example (Frame A). As shown in Fig. (9), the fourth story of this frame has only three bays. All panels of this frame have infill walls except the first story second panel (between gridlines 2 and 3), which is the entrance to the building. The other three panels of the first story have full infill walls, while the next three stories are partially infilled. A total gravity load of 150 psf (7.18 kN/m²) is considered for all levels.

Masonry infill walls with 8 in. (203 mm) thickness and masonry compressive strength of 2500 psi (17.25 MPa) is considered for all panels. The main purpose of this example is to show the design procedure in a more realistic example with varying conditions such as story height, panel lengths, and panels with no infill or partial infill walls. Seismic design loads are shown in Fig. (10) for Frame A. For this four-story frame, since the sizes of walls are not the same in all bays, the simplified design procedure presented in the previous example needs to be generalized. The design procedure, which is subsequently explained, is a general method and can be used for any multi-bay, multi-story building with par-

tial infill and full infill walls in some or all panels and different story and bay sizes.

First, the capacity of the masonry wall in each panel is estimated with the use of Eq. (7). In this equation, the tensile strength of masonry is assumed to be 5% of the compressive strength of masonry resulting in a tensile strength of 125 psi (0.86 MPa). The resulting capacities for masonry walls are included in Fig. (10) for each panel. Next, the stiffness of each wall needs to be determined. The total deflection of the frame at each floor level is the sum of the deflection of the wall and the deflection of the column above the wall (along the free length of the column). The in plane stiffness associated with the wall deflection, K_{wall} , and frame (column) deflection, K_{frame} , are calculated according to Eqs.(12) and (13), respectively, for each panel and the total stiffness for the panel, K_{total} , is calculated as Eq. (14). Fig. (11) shows the diagrammatic design procedure and the summary of calculations for this example.

$$K_{wall} = \frac{E_m t}{4 \left(\frac{h}{L}\right)^3 + 3 \left(\frac{h}{L}\right)} \tag{12}$$

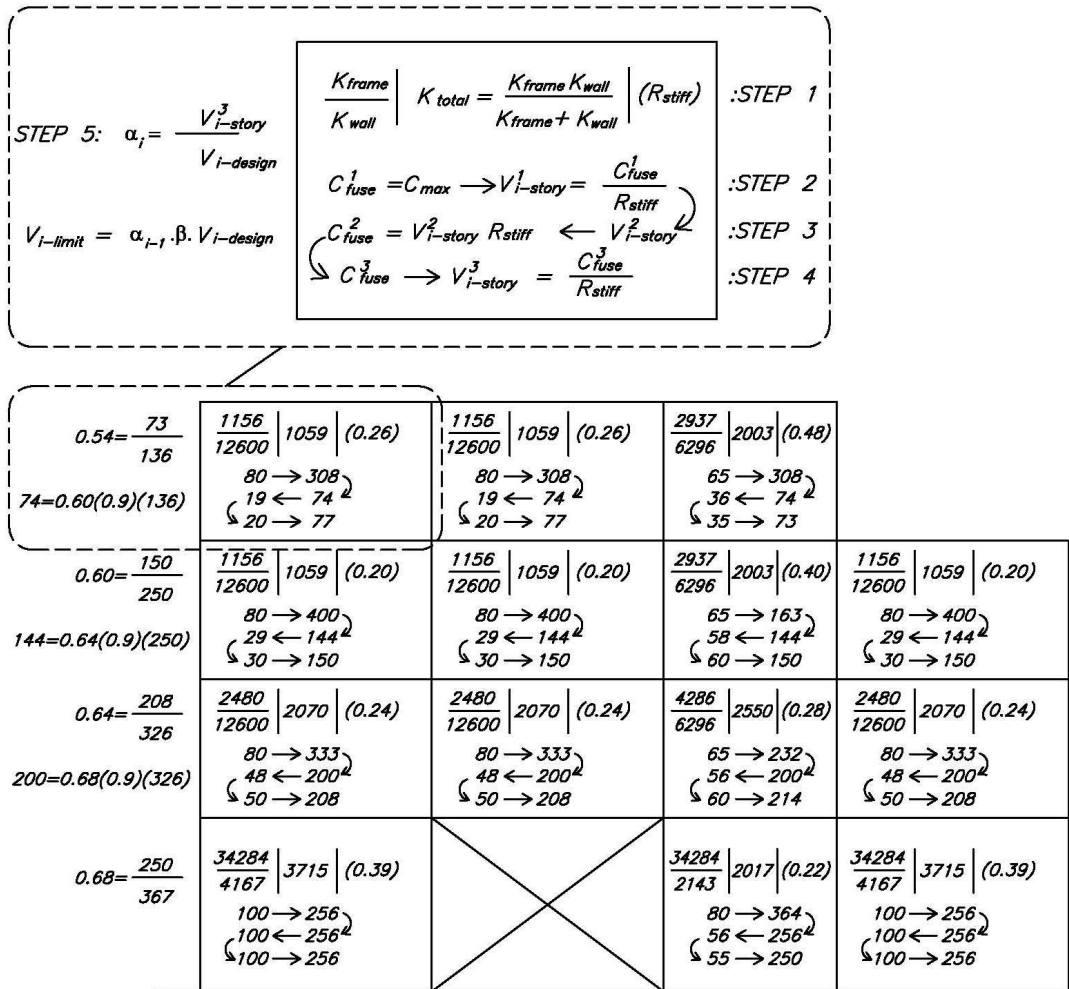


Fig. (11). Calculations for four-story building example (1 kip = 4.448 kN).

$$K_{frame} = \frac{12E_{fr}I}{h^3} \text{ for fixed-end, } K_{frame} = \frac{3E_{fr}I}{h^3} \text{ for free-end (13)}$$

$$K_{total} = \frac{1}{\frac{1}{K_{wall}} + \frac{1}{K_{frame}}} \text{ (14)}$$

The calculation related to each panel is shown on that panel in Fig. (11). The top part of this figure presents the parameters and formulations used for each panel as a guide. The wall, frame, and total stiffness are included in the top part of each panel. The ratio of the resulting stiffness of each panel to the total stiffness of the story is calculated and listed in parenthesis for each panel (Step 1). In the lower part of each panel in Fig. (11), there are two columns. The first column presents the capacity of the fuse element, in which the first number, C_{fuse}^1 , (top number) is the capacity of the wall (maximum allowed capacity of fuse element) as the first trial; the second number, C_{fuse}^2 , (middle number) is the second trial; and the third number, C_{fuse}^3 , (bottom number) is the third trial (the final design) for fuse element capacity. The second column represents the story shear resistance associated with the trial fuse element capacity.

The design of fuse element's capacity starts from the first story and continues to the top story (from bottom to top). For the first story, initially, for each panel, the maximum allowable capacity of fuse element is considered as the first trial, C_{fuse}^1 . The story shear resistance associated with this capacity, V_{story}^1 , is calculated using Eq. (15) and listed as the first number of the second column (Step 2).

$$V_{story}^1 = \frac{C_{fuse}^1}{R_{stiff}} \text{ (15)}$$

In the next step, the second trial for story shear, V_{story}^2 , is selected to be the minimum of (1) V_{story}^1 of the four panels of the first story and (2) the story design shear force. The capacity of the fuse element associated with this story shear is calculated using Eq. (16) and listed as the second number, C_{fuse}^2 , for each panel (Step 3).

$$C_{fuse}^2 = V_{story}^2 \times R_{stiff} \text{ (16)}$$

The third trial of fuse element capacity, C_{fuse}^3 , is chosen as the final design. For this purpose, it is assumed that the grades of fuse elements are increasing in increments of 5 kips (22 kN). Thus, if a capacity of 48 kips (213 kN) is calculated for C_{fuse}^2 , C_{fuse}^3 is taken as 50 kips (222 kN). Similarly, the story shear associated with this capacity is calculated as Eq. (17) (Step 3).

$$V_{story}^3 = \frac{C_{fuse}^3}{R_{stiff}} \text{ (17)}$$

The smallest value of V_{story}^3 for the four panels of each story is the final story shear resistance. Lastly, the ratio of the story shear resistance to story shear force (α) is calculated and listed in the top left side of each story (Step 5). This procedure is applied for the rest of the stories from bottom (the 2nd story) to top (the 4th story). The only difference between the procedure for the first story and the other stories is that in Step 2, V_{story}^2 is the smallest value of: (1) V_{story}^1 of the panels; (2) the story design shear force, and (3) $V_{i-limit}$ as defined in Eq. (18), in which, $V_{i-design}$ is the story design shear force, α_{i-1} is the ratio of story shear resistance to story shear force of the lower story, and β_i is a coefficient smaller than unity that controls the sequence of the crushing of fuse elements in elevation per designer's choice. A value of 1.0 for β_i causes simultaneous crushing of fuse elements of the two stories. On the other hand, very small values for β_i result in lower fuse element capacities for stories above, which will be inefficient. Thus, it is recommended to select a number between 0.85 and 0.95 for β_i .

$$V_{i-limit} = \alpha_{i-1} \times \beta_i \times V_{i-design} \text{ (18)}$$

The designed fuse elements are listed in Table 3 (3rd columns). The α_i ratios (6th column in Table 3) show that the sequence of crushing is from top to bottom with increasing values of α_i ratios. It is 0.54, 0.60, 0.64, and 0.68 for the 4th, 3rd, 2nd, and 1st stories, respectively. Similar to the previous example, the results and advantages of fuse system can be

Table 3. Four-story Building Design Example

Story	Story Shear kip (KN)	Fuse Element Capacity-kip (KN)				Story Shear Capacity Kip (KN)	Story Capacity / Story Shear	Fuse Crushing Sequence
		1 st Bay	2 nd Bay	3 rd Bay	4 th Bay			
(1)	(2)	(3)	(3)	(3)	(3)	(4)	(5)	(6)
4	136 (605)	20 (89)	20 (89)	35 (156)	NA	73 (325)	0.54	1
3	250 (1112)	30 (133)	30 (133)	60 (267)	30 (133)	150 (667)	0.60	2
2	326 (1450)	50 (222)	50 (222)	60 (267)	50 (222)	208 (925)	0.64	3
1	367 (1632)	100 (445)	NA	55 (245)	100 (445)	250 (1112)	0.68	4

discussed for this example as well. However, this example is limited to presentation of application of design approach and process.

CONCLUDING REMARKS

A design approach was presented for the proposed infill wall fuse system. This included the use of empirical equations for the design and prediction of the in-plane strength of masonry infill walls equipped with the structural fuse system; sizing and specifying the capacity arrangement for fuse elements in multi-bay multi-story frame buildings, and design checks for induced concentrated loads on structural frames due to their interaction with fuse device. The suggested design approach was then illustrated as applied to two building examples: a low-rise (four-story) and a mid-rise (eight-story) building in high seismic zone of Los Angeles, CA. It should be mentioned that these results are based on static load application and that the lateral load distribution can change in actual dynamic load application. Follow-up work is needed to refine the proposed design approach for situation when cyclic and dynamic loading is applied to the system.

Based on the study reported in this paper the following remarks can be made:

(1) The proposed design approach can determine the appropriate capacity (grade) arrangement for infill wall fuse elements in elevation and in bays with different geometry and conditions to achieve a suitable sequence of crushing of fuse elements and eliminate development of soft-story mechanisms. The proposed process can be programmed and included into the finite element programs used in structural analysis and design.

(2) For efficient use of masonry wall in-plane strength and stiffness in a system equipped with fuse elements, the in-plane flexural induced uplift failure of wall should be eliminated. This can be done by providing adequate strength for the vertical tie-down element.

(3) Crushing of fuse elements in a building structure depends on several parameters including intensity of earthquake, strength and stiffness properties of masonry walls and geometrical parameters of the building (*i.e.*, wall and panel sizes). Based on the results of the two examples discussed in this paper, the following statements can be made for typical buildings:

- a) In typical low-to-mid rise buildings in low seismic zones, the fuse elements may not crush. Thus, the designer may choose to use traditionally integrated masonry infill walls. However, it is always safe to use the fuse-like elements to ensure safety for a more conservative design or for performance-based approach (*i.e.*, damage to be minimized). Furthermore, the designer can alternatively decide to use lighter or weaker masonry walls with an infill wall fuse system, which can lower the construction cost while maintaining the structural performance.
- b) In typical low-rise buildings in high seismic zones, some or all of the fuse elements are expected to crush.

- c) For typical mid-to-high rise buildings in high seismic zones, all of the fuse elements are expected to crush.
- d) Minor-to-moderate earthquakes may cause the crushing of some or all of the fuse elements in high rise buildings.

(4) In the analysis and design of the confining frame equipped with infill wall fuse system, its interaction with the infill wall panel before crushing of fuse elements needs to be taken into account (global effects). The confining frame needs to be checked for the induced concentrated compression and tensile forces due to interaction with fuse device (local effects).

(5) The proposed fuse system can be used for seismic retrofit and upgrade of existing and old buildings as well as in new constructions.

It should be mentioned that the specific actions of design procedure presented in this paper one meant to be used for fuse system with rigid-brittle elements only. However the concept and approaches can be expanded and utilized for systems incorporating fuse elements with alternative design (*i.e.*, fuse element with spring or dashpot components). The structure and details of fuse concept are not commercially developed yet. The protection of the fuse element against environmental effects and possible material deterioration shall be considered when providing detail for final development of the system.

CONFLICT OF INTEREST

The authors confirm that this article content has no conflicts of interest.

ACKNOWLEDGEMENTS

Partial funding for this study was provided by the National Science Foundation under Grant Number CMS-9983896. The support of National Science Foundation is gratefully acknowledged. The views expressed in this paper are those of the authors and do not necessarily represent those of the National Science Foundation.

NOTATION

The following symbols are used in this paper:

A	=	cross section area of wall
A_e	=	effective area of masonry wall
A_{sh}	=	horizontal steel area
A_{sv}	=	vertical steel area
C_i	=	the Shing <i>et al.</i> [23] equation constants ($i=1, 2, 3, 4, 5$)
C_{ij}	=	capacity of fuse element in story i and bay j
C_{max}	=	maximum capacity of fuse element
C_{rh}	=	horizontal steel capacity reduction factor
C_{fuse}^j	=	fuse element capacity trial j
E_{fr}	=	modulus of elasticity of frame
E_m	=	modulus of elasticity of masonry wall

F_i	=	applied lateral load at floor level i	f_m^*	=	compressive strength of masonry
H	=	total height of wall panel	f_t	=	tensile strength of masonry
I	=	moment of inertia of frame	f_{yh}	=	horizontal steel yield strength
K_{frame}	=	in-plane stiffness of frame	h	=	elevation of applied in-plane load (location of fuse element)
K_{wall}	=	in-plane stiffness of masonry wall	h'	=	elevation of center of horizontal compression stress at wall corner
K_{total}	=	in-plane stiffness of infilled frame	k_o, k_u	=	constants equal to 1.0 for fully grouted masonry wall
L	=	total length of wall panel	l	=	horizontal distance between tie-down element and jamb
M_n	=	nominal flexural strength of wall	l'	=	horizontal distance between center of compression stress and jamb
N	=	vertical tie-down load	r	=	wall aspect ratio = H/L
R	=	lateral force-resisting system over strength coefficient	s	=	spacing of horizontal steel
R_{stiff}	=	relative stiffness of each bay in story	t	=	thickness of wall
SF	=	safety factor	Φ_h	=	horizontal steel capacity reduction factor
V	=	nominal shear strength of wall	α_i	=	ratio of story shear resistance to story shear force
V_m	=	shear resistance contribution of masonry	α_v	=	wall shear ratio = $\psi' r$
V_p	=	shear resistance contribution of axial compression	β	=	h/l
V_{sh}	=	shear resistance contribution of horizontal steel	β_i	=	fuse element sequence control factor in story i
V_{sv}	=	shear resistance contribution of vertical steel	δ	=	1.0 for fixed ends walls, 0.6 for cantilever walls
$V_{i-story}^j$	=	story shear resistance due to fuse element story i trial j	γ	=	constant equals to 1.0 for fully grouted masonry wall
$V_{i-design}$	=	story i design shear force	κ	=	stress distribution factor (= 0.85 for equivalent rectangular stress block method)
V_{i-reqd}	=	Applied/required shear force at story i	ρ_h	=	horizontal steel ratio
$V_{i-brace}$	=	resistance of brace at story i	ρ_v	=	vertical steel ratio
$V_{i-frame}$	=	resistance of frame at story i	σ_c	=	axial compressive stress
V_{i-wall}	=	resistance of masonry wall at story i	τ_o	=	cohesion
$V_{i-total}$	=	total resistance of infilled frame at story i	ψ	=	wall aspect ratio coefficient in NEHRP [31] equation = $0.96-0.68\text{Log}(r)$
$V_{i-limit}$	=	limiting shear resistance for story i	ψ'	=	0.5 for fixed ends walls, 1.0 for cantilever walls
b	=	shear stress distribution factor = 1.5 for $r \geq 1.5$, 1.0 for $r \leq 1.5$, r for $1.5 \geq r \geq 1.0$			
c_1	=	$0.0018 / \sqrt{psi}$			
c_2	=	$2.0 \sqrt{psi}$			
c_3	=	$1.0 \sqrt{psi}$			
d	=	effective depth of wall			
d'	=	the centroidal distance of the vertical steel to the nearest jamb			
d_{rv}	=	diameter of a single vertical steel			
f_m	=	compressive strength of embedding mortar or grout			

REFERENCES

- [1] R.G. Drysdale, and A.A. Hamid, *Masonry Structures – Behavior and Design*, 3rd ed. The Masonry Society, Boulder: Colorado, 2008.
- [2] T. Paulay, and M. J. N. Priestley, *Seismic Design of Reinforced Concrete and Masonry Buildings*. Wiley, USA, 1992.
- [3] NISEE, *National Information Service for Earthquake Engineering*. University of California, Berkeley, CA, 1997.

- [4] M. Çelebi, P. Bazzurro, L. Chiaraluce, P. Clemente, L. Decanini, A. DeSortis, W. Ellsworth, A. Gorini, E. Kalkan, S. Marcucci, G. Milana, F. Mollaioli, M. Olivieri, R. Paolucci, D. Rinaldis, A. Rovelli, F. Sabetta, and C. Stephens, "Recorded motions of the 6 april 2009 mw 6.3 l'aquila, italy, earthquake and implications for building structural damage: overview", *Earthquake Spectra*, vol. 26, no. 3, pp. 651-684, 2010.
- [5] R.O. Hamburger and J.D. Meyer, "The performance of steel-frame buildings with infill masonry walls in the 1906 san francisco earthquake," *Earthquake Spectra*, vol. 22, no. S2, S43-S67, 2006.
- [6] M. Tomazevic, *Earthquake-Resistant Design of Masonry Buildings*. Imperial College Press London, UK, 1999.
- [7] D. J. Dowrick, *Earthquake Resistant Design for Engineers and Architects*, 2nd ed. Wiley, USA, 1987.
- [8] A.M. Memari, and M. Aliaari, "Seismic infill wall isolator subframe (SIWIS) system for use in buildings," *Proceeding of ATC-17-2 Seismic on Response Modification Technologies for Performance-Based Design*, Los Angeles: USA, 2002.
- [9] M. Aliaari, "The development of seismic infill wall isolator subframe (siwis) system for use in buildings," Ph.D. thesis, The Pennsylvania State University, University Park, PA, 2005.
- [10] M. Aliaari, and A. M. Memari, "Analysis of masonry infilled steel frames with seismic isolator subframes", *Eng. Struct. J.*, vol. 27, pp. 487-500, 2005.
- [11] M. Aliaari, and A. M. Memari, "Experimental evaluation of a sacrificial seismic fuse device for masonry infill wall," *ASCE J. Architect. Eng.* vol. 13, no. 2, pp. 111-125, 2007.
- [12] C.K. Seah, "A universal approach for the analysis and design of masonry infilled frame structures," PhD thesis, University of New Brunswick, Fredericton, N.B., Canada, 1998.
- [13] A. Stavridis, and P.B. Shing, "Calibration of a numerical model for masonry infilled rc frames," *The 14th World Conference on Earthquakes Engineering*, Beijing, China, 2008.
- [14] G. Milani, "3D upper bound limit analysis of multi-leaf masonry walls," *Int. J. Mechan. Sci.* vol. 50, no. 4, pp. 817-836, 2008.
- [15] W.W. El-Dakhakhni, M. Elgaaly, A.A. Hamid, "Three-strut model for concrete masonry-infilled steel frames," *J. Struct. Eng. ASCE*, vol. 129, pp. 177-185, 2003.
- [16] J.M. Blondet, R.A. Mayes, T.V. Kelley, F. Ricardo, and R.E. Klinger, "Performance of engineered masonry in the chilean earthquake of march 3, 1985: implementations for u.s. design practice," Phil Ferguson Structural Engineering Laboratory, University of Texas, Austin, Texas, 1989.
- [17] J.D. Brunner, and P.B. Shing, "Shear strength of reinforced masonry walls," *Mason. Soc. J.*, pp. 65-77, 1996.
- [18] S.G. Fattal, *Strength of Partially-Grouted Masonry Shear Walls under Lateral Loads*. NISTIR 5147, National Institute of Standards and Technology, Gaithersburg, MD, 1993.
- [19] E.G. Kurt, B. Binici, O. Kurc, E. Canbay, Akpınar, and G. Özcebe, "Seismic Performance of a Deficient Reinforced Concrete Test Frame with Infill Walls," *Earthquake Spectra.*, vol. 27, no. 3, pp. 817-834, 2011.
- [20] G. Mondal, and S.K. Jain, "Lateral stiffness of masonry infilled reinforced concrete (rc) frames with central opening," *Earthquake Spectra.*, vol. 24, no. 3, pp. 701-723, 2008.
- [21] G. Magenes, and G.M. Calvi, "In-plan seismic response of brick masonry walls," *Earthquake Eng. Struct. Dyn.*, vol. 26, pp. 1091-1112, 1997.
- [22] A. Matsumura, "Effect of Shear Reinforcement in Concrete Masonry Walls," *1st Meeting of the U.S.-Japan Joint Technical Coordinating Committee on Masonry Research*, Tokyo: Japan, 1985.
- [23] A. Matsumura, "Shear Strength of Reinforced Hollow Unit Masonry Walls," *Proceeding of the 4th North American Masonry Conference*, Report No. 50, Los Angeles: USA, 1987.
- [24] A. Matsumura, "Effectiveness of Shear Reinforcement in Fully Grouted Hollow Clay Masonry Walls," *4th Meeting of the U.S.-Japan Joint Technical Coordinating Committee on Masonry Research*, San Diego: USA, 1988.
- [25] A. Matsumura, "Shear Strength of Reinforced Masonry Walls," *Proceeding of the 9th World Conference on Earthquake Engineering, VI*, Tokyo-Kyoto: Japan, 1988.
- [26] P.B. Shing, M. Schuller, V.S. Hoskere, and E. Carter, "Flexural and Shear Response of Reinforced Masonry Walls," *ACI Struct. J.*, vol. 87, no. 6, pp. 646-656, 1990.
- [27] P.B. Shing, J.D. Brunner, and H.R. Lotfi, "Evaluation of shear strength of reinforced masonry walls," *Mason. Soc. J.*, pp. 61-76, 1993.
- [28] M. Tomazevic, and M. Lutman, "Seismic Resistance of Reinforced Masonry Walls," *Proceeding of the 9th World Conference on Earthquake Engineering, VI*, Tokyo-Kyoto: Japan, 1988.
- [29] *Uniform Building Code*, International Conference of Building Officials, Whittier: USA, 1997.
- [30] Eurocode 6, *Design of Masonry Structures, Part 1: General Rules for Buildings, Rules for Reinforced and Unreinforced Masonry*, CEN, Berlin: Germany, 1996.
- [31] NEHRP, *Recommended Provisions for the Development of Seismic Regulations for New Buildings and Other Structures, Part 1, Provisions*, Federal Emergency Management Agency (FEMA), 2000.
- [32] ICC, *2006 International Building Code*. International Code Council, Inc, 2006.
- [33] Building Code Requirements for Masonry Structures, *ACI 530-05/ASCE 5-05/TMS 402-05*. Masonry Standards Joint Committee (MSJC), 2005.
- [34] D.P. Abrams, "Masonry as a Structural Material," *Proceedings of the Materials Engineering Congress, Materials Engineering Division*. ASCE, Atlanta: USA, pp. 116-129, 1992.
- [35] L. Guiqiu, S. Chuxian, and B. Jinlin, "The Shear Strength of Unreinforced Masonry Wall," *Proceeding of the 11th International Brick/Block Masonry Conference*, Tongji University, Shanghai, 1997.
- [36] ASCE 7, *Minimum Design Loads for Buildings and Other Structures*, American Society of Civil Engineers, Reston: USA, 2002.
- [37] H.B. Kaushik, D.C. Rai, and S.K. Jain, "Code Approaches to Seismic Design of Masonry-Infilled Reinforced Concrete Frames: A State-of-the-Art Review," *Earthquake Spectra.*, vol. 22, no. 4, pp. 961-983, 2006.

Received: October 01, 2012

Revised: October 23, 2012

Accepted: October 28, 2012

© Aliaari and Memari; Licensee Bentham Open.

This is an open access article licensed under the terms of the Creative Commons Attribution Non-Commercial License (<http://creativecommons.org/licenses/by-nc/3.0/>) which permits unrestricted, non-commercial use, distribution and reproduction in any medium, provided the work is properly cited.